Covalent incorporation of the surfactant into high internal phase emulsion templated polymeric foams

Sebastijan Kovačič,[a,*] Florian Preishuber-Pflügl,[b] David Pahovnik,[a] Ema Žagar,[a] Christian Slugovc[b,*]

[a] *Laboratory for Polymer Chemistry and Technology, National Institute of Chemistry, Hajdrihova 19, 1000 Ljubljana, Slovenia.*

[b] *Graz University of Technology, Institute for Chemistry and Technology of Materials (ICTM), NAWI Graz, Stremayrgasse 9, 8010 Graz, Austria.*

Electronic Supplementary Information

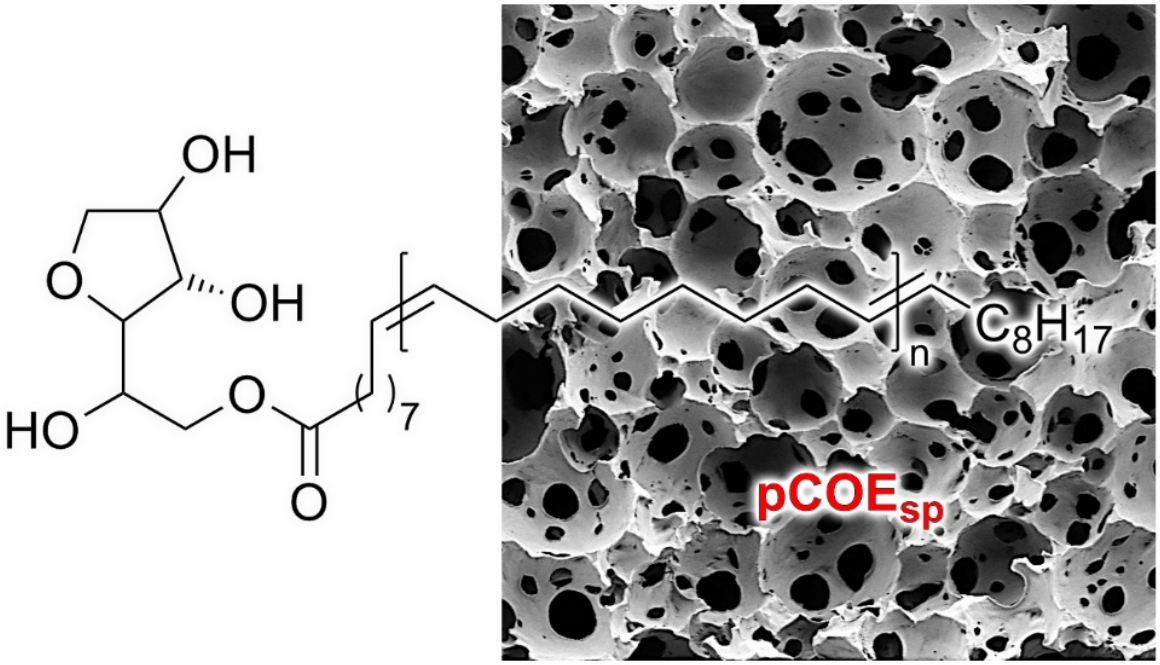

Experimental

Cyclooctene (*Sigma-Aldrich*, amounts according to Table S1) and surfactants (Pluronic L-121: Poly(ethylene glycol)-*block*-poly(propylene glycol)-*block*-poly(ethylene glycol); M_W = 4400 $gmol^{-1}$; Span 80: Sorbitan monooleate; M_W= 428 $gmol^{-1}$, all *Sigma-Aldrich*) were placed in a three necked 250 mL flask and the mixture was stirred with an overhead stirrer at 400 rpm. The corresponding amount (*cf*. Table S1) of deionised water was added drop-wise under constant stirring. After addition of water the mixture was further stirred for 1 h until a uniform emulsion was produced. Then, 100 µL solution **M20** initiator (H_2IMes)(PPh_3)Cl_2Ru(3-phenylinden-1-ylidene) (H_2Imes = *N*,*N*-bis(mesityl) 4,5-dihydroimidazol-2-yl); *cf*. Figure S1) in toluene was added to the emulsion, and the mixture was stirred for further 1 min. Subsequently, the emulsion was transferred to the mould and cured for 24h at room temperature (solidification was noted already after approx. 15 min). The resulting polymers were purified via Soxhlet extraction with acetone and dried under vacuum until constant weight was obtained.

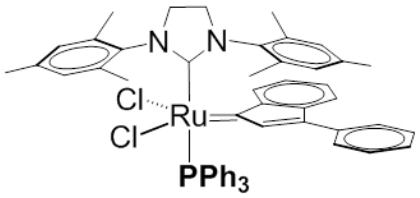

M20

Figure S1. Ru-indenylidene based initiator with triphenylphosphin as co-ligand.

Table S1. Emulsion composition (80 vol% aqueous phase)

	COE		Sp 80	PL121	H_20	M20	
sample	V [mL]	n [mol]	V [mL]	m [g]	V [mL]	m [mg]	**M20:COE**
$pCOE_{sp10}$	2.2384	0.01830	0.2842	/	9.0	5.5	1 : 2911
$pCOE_{sp20}$	2.3758	0.02160	0.5851	/	9.5	5.8	1 : 2931
$pCOE_{sp30}$	2.3750	0.02159	1.0112	/	9.5	5.8	1 : 2931
$pCOE_{pl10}$	2.3846	0.02167	/	0.3002	9.6	5.7	1 : 2995

FTIR

The FT-IR spectra were recorded on a Perkin-Elmer Spectrum One instrument (Perkin-Elmer, Inc., USA) upgraded with Universal ATR Accessory with diamond Top-plate-ZnSe. Spectra were recorded in the range of 650–4000 cm^{-1} at a resolution of 4 cm^{-1}. Data acquisition and processing was done with PE Software Spectrum.

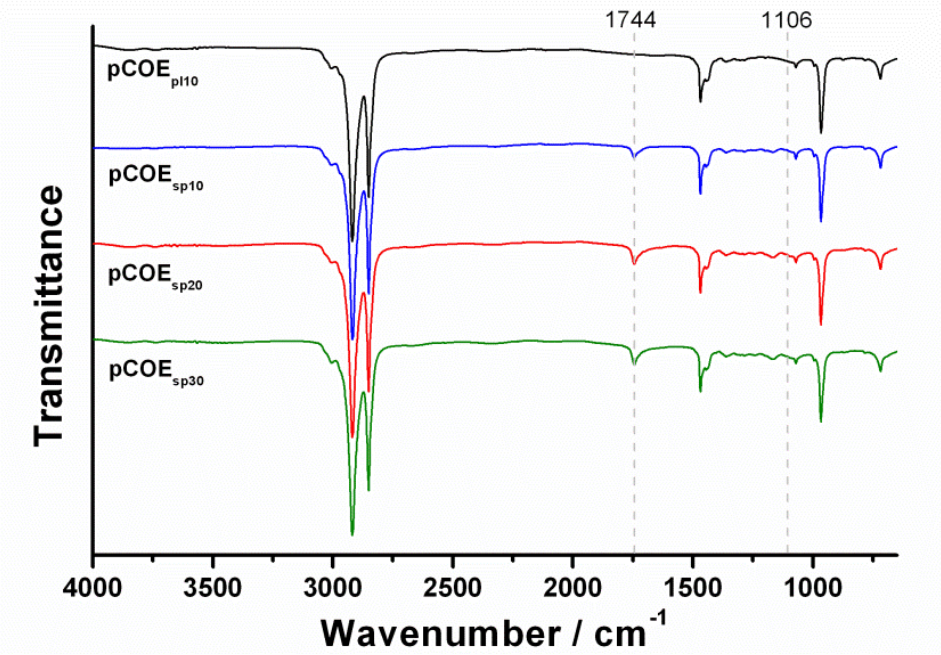

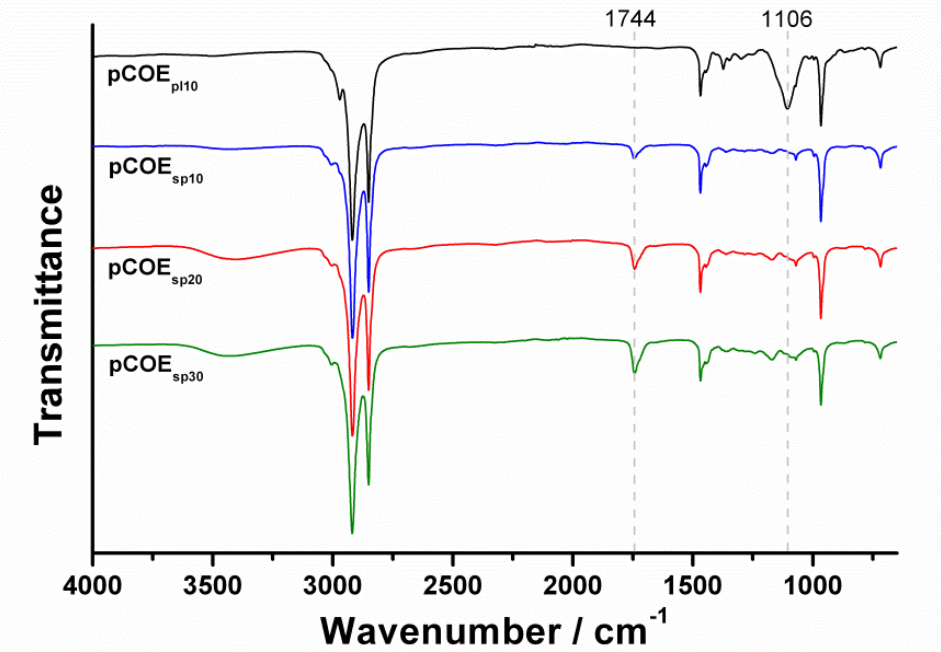

Figure S2. FTIR spectra of purified (above) and raw **pCOE** samples (below).

NMR

The ^{1}H NMR spectra of samples were recorded in $CDCl_3$ on a 300-MHz Agilent Technologies DD2 spectrometer in the pulse Fourier Transform mode with both a relaxation delay and an acquisition time of 5 s. Tetramethylsilane (TMS) was used as the internal chemical-shift standards. Signals from 3.4 - 3.6 and at 1.13 ppm confirm the presence of residual Pluronic in the corresponding sample.

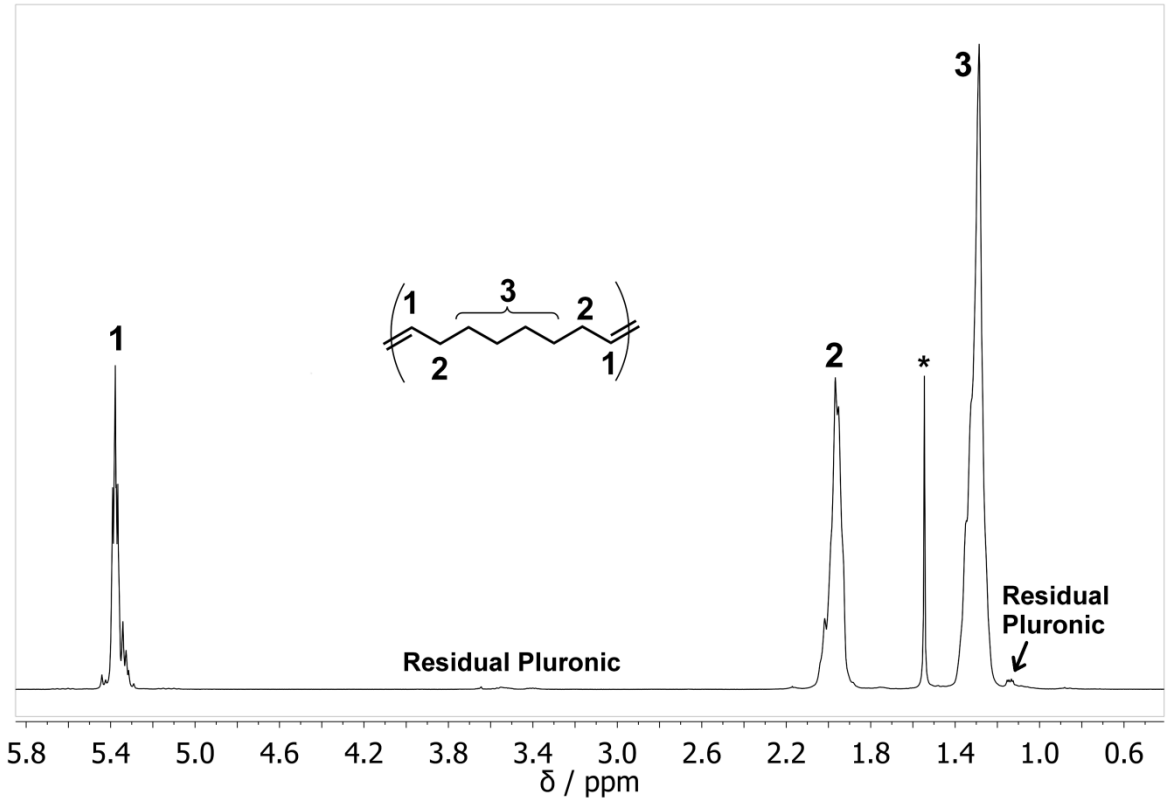

Figure S3. NMR spectrum of **pCOE$_{pl10}$** sample.

Size-exclusion chromatography (SEC- MALS)

The separations of original and purified samples by SEC were carried out in chloroform using an Agilent 1200 HPLC pump and MIXED-E (7.5 mm × 300 mm, molar mass range up to 30 kDa, Agilent Technologies) and Oligopore (7.5 mm × 300 mm, molar mass range up to 4,5 kDa, Polimer Laboratories) analytical columns connected in series. For the detection, we used a multi-angle light-scattering (MALS with 18 angles) detector (DAWN-HELEOS, Wyatt Technology Corp.) and an interferometric refractive index (RI) detector (Optilab rEX, Wyatt Technology Corp.). The nominal eluent flow rate was 0.8 mL/min, the injection volume was typically 100 μL, and the mass of the samples injected onto the column was typically 150 μg.

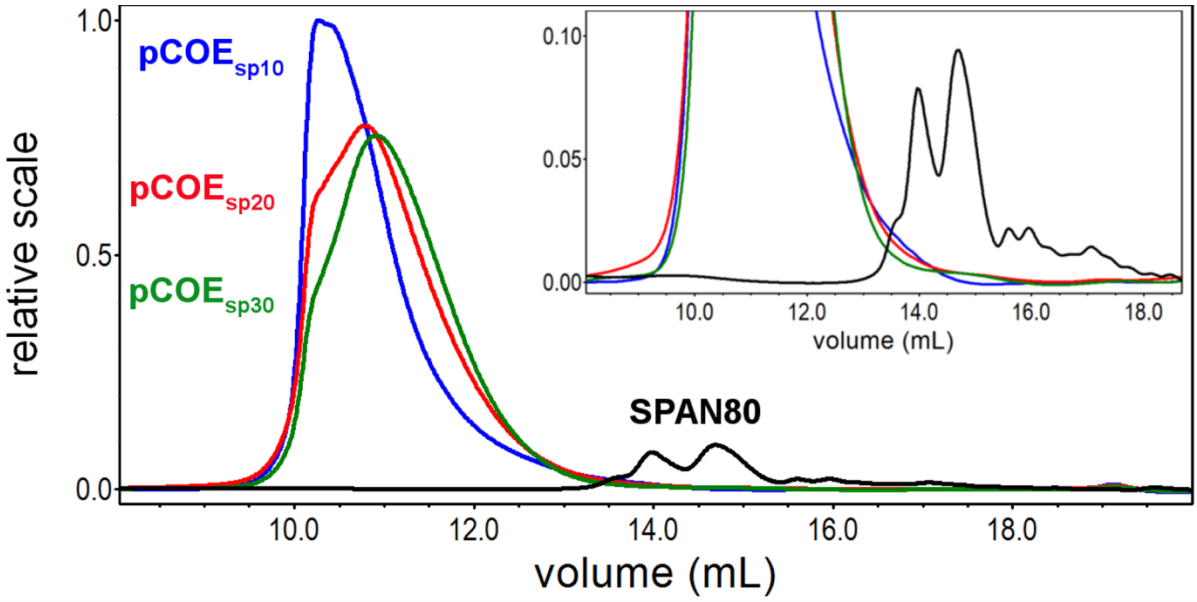

Figure S4. SEC-RI chromatograms of purified pCOE samples (**blue – pCOE$_{sp10}$, red – pCOE$_{sp20}$, green – pCOE$_{sp30}$ and black – pure Span 80).**

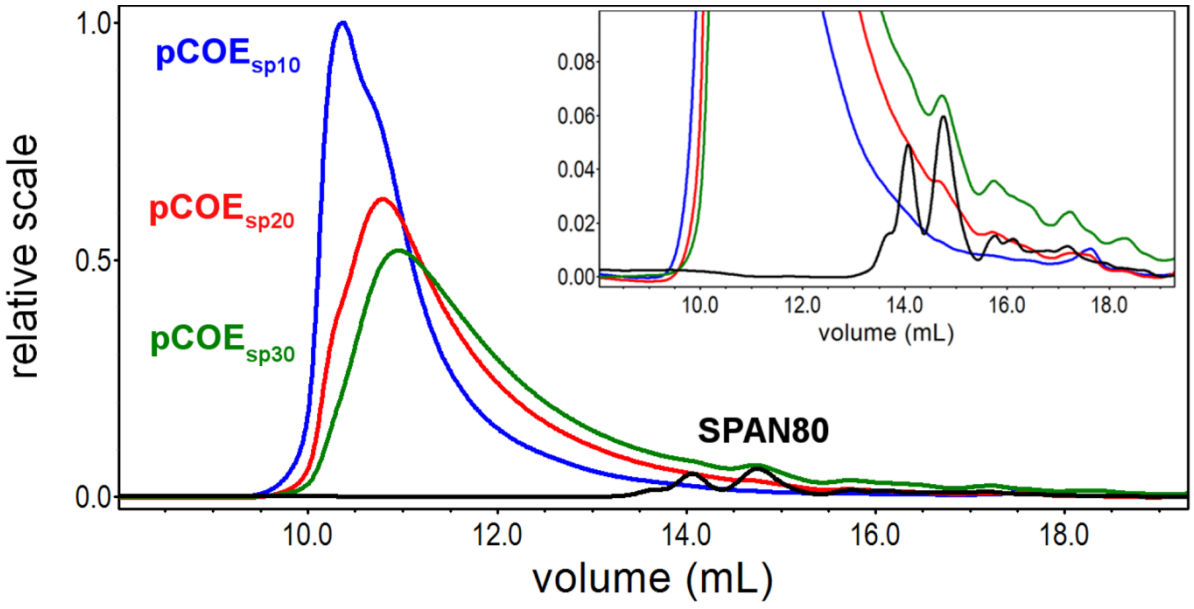

Figure S5. SEC-RI chromatograms of raw pCOE samples (**blue – pCOE$_{sp10}$, red – pCOE$_{sp20}$, green – pCOE$_{sp30}$ and black – pure Span 80).**

MALDI-TOF MS

Matrix-assisted laser desorption/ionization time-of-flight mass spectrometric (MALDI-TOF MS) measurements were performed on a Bruker Ultraflex III MALDI-TOF mass spectrometer (Bruker Daltonik, Bremen, Germany). Samples were dissolved in THF (10 mg mL^{-1}) and 1 µL was mixed with 10 µL of matrix solution, dithranol in THF (20 mg mL^{-1}), followed by the

addition of 0.5 μL of Ag(trifluoroacetate) in THF (10 mg mL^{-1}) as a cationizer. Then, 0.4 μL of the final solution was spotted on the target plate (dried-droplet method). The reflective positive ion mode was used to acquire the mass spectra of samples. The calibration was made externally with the poly(methyl methacrylate) standards using the nearest-neighbour positions.

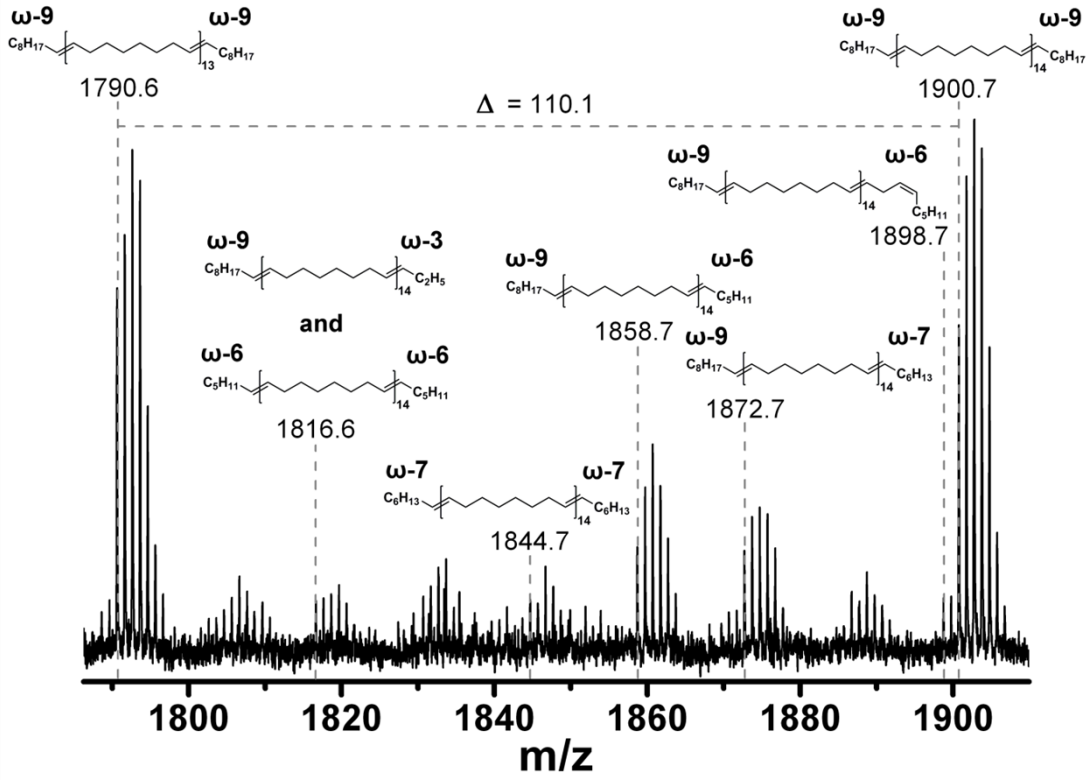

Figure S6. Magnification of the figure shown in the manuscript.

Since $pCOE_{sp}$ samples have broad molar mass distribution only the signals of low molecular weight species were observed in MALDI-TOF mass spectra. The distance between the signals of 110.1 Da was determined, which fits exactly to the molecular weight of pCOE repeating unit. In addition to the main signal distribution several distributions of lower intensity were observed, showing the presence of pCOE macromolecules with different end-groups. The signals of the main distribution correspond to the macromolecules with alkyl end-groups formed by the cross-metathesis reaction with the oleate tails (ω-9), which represents the major share of Span 80. Lower intensity peak distributions are due to the cross-metathesis reaction with the ω-6, ω-7 and ω-3 unsaturated fatty acid tails of Span 80 and results in pCOE of different lengths of the alkyl end-groups (Figure 2F). Unfortunately, we were not able to detect the signals of pCOE with sorbitan moiety as the chain end-groups in MALDI-TOF

mass spectra. This was ascribed to the fact that Span 80 is a mixture of mono- (32 %), di- (36 %), tri- (20 %) and tetraesters (6 %), [Z. Wang and M. Fingas, *J. High Resolut. Chrom.*, 1994, **17**, 15-19; Z. Wang and M. Fingas, *J. High Resolut. Chrom.*, 1994, **17**, 85-90.], which after cross-metathesis reaction leads to a significantly higher number of possible sorbitan containing chain end-groups as compared to their alkyl terminated counterparts. As a consequence of this fact, also the intensity of the signals due to the species containing sorbitan end-groups is much lower.

Specific surface area and skeletal density measurements

Specific surface area of the samples was determined from the adsorption and desorption isotherms of N_2 at -196 °C using a Micromeritics TriStar II 3020 instrument. These experiments were performed after degassing the samples under N_2 stream (purity 6.0) and heating at 40°C for 240 min. The specific surface area of the samples was calculated by applying the BET theory to the nitrogen adsorption data within the 0.06 - 0.30 P/P_0 range. Skeletal density of samples investigated in the present study was evaluated using a fully automated and high-precision helium pycnometer (Micromeritics, model AccuPyc II 1340). Prior to measurements the samples were thoroughly dried and purged in order to exclude the influence of moisture and adsorbed impurities on the measured data. The reported values of skeletal density represent an average of ten consecutive measurements.

Scanning Electron Microscopy (SEM) investigations

Morphology investigations of samples were performed by a scanning electron microscopy. SEM images were taken on a Field emission electron microscope Ultra+ (Carl Zeiss) equipped with an energy dispersive spectrometer SDD X-Max 50 (Oxford Instruments). A piece of each sample was mounted on a carbon tab for better conductivity and a thin layer of gold was sputtered on sample surface prior scanning analysis. An average void size was determined from SEM micrographs analysis after scanning. Therefore, the mean and the standard deviations were drawn by manual measurements of diameters from a population of at least 40 voids. To get a better estimation of the real void diameter, it is necessary to introduce a statistical correction. Multiplication of the observed voids values from SEM images by a statistical factor of $2/3^{1/2}$ allows for a better estimation of the real cavity diameters [A. Barbetta and N. R. Cameron, *Macromolecules*, 2004, **37**, 3188-3201].

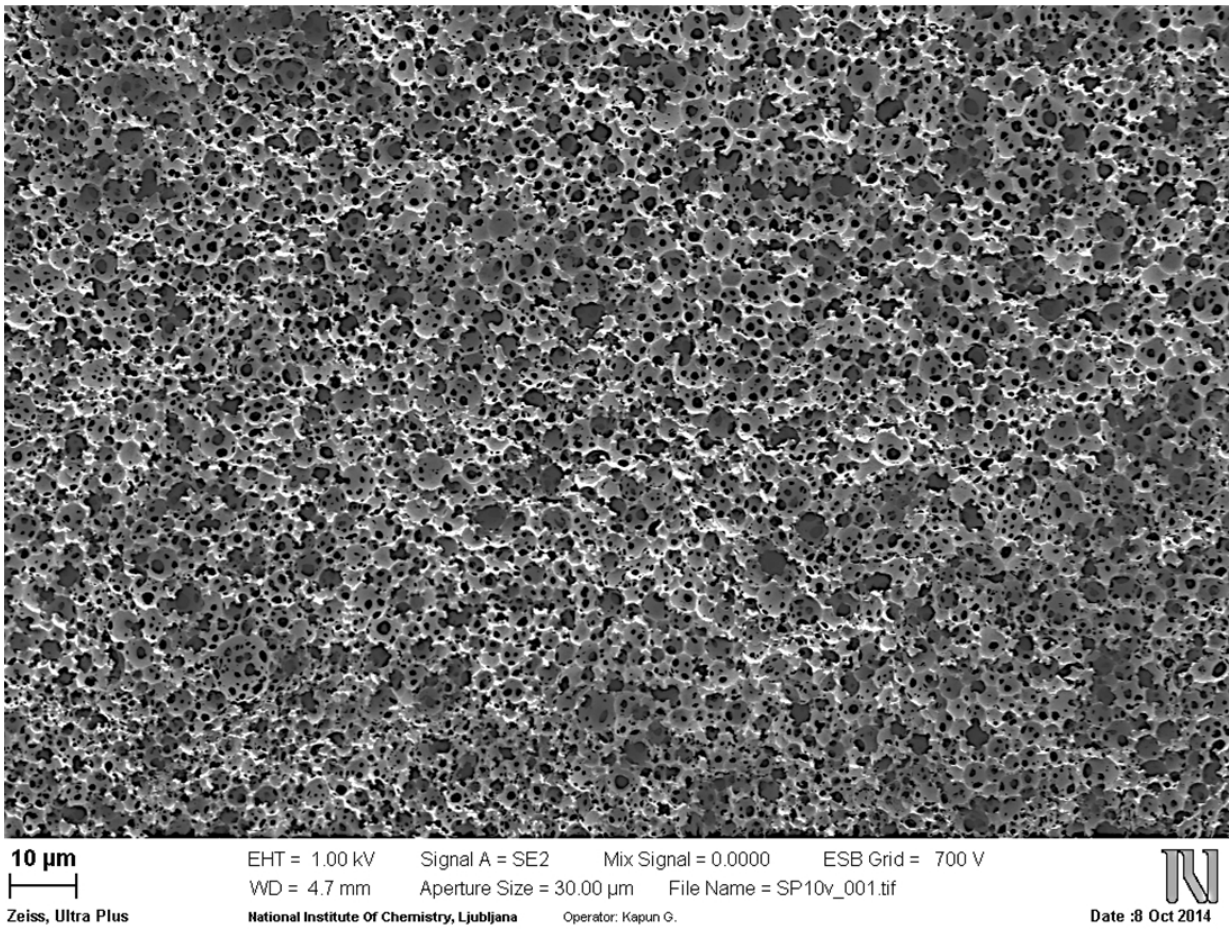

Figure S7. SEM image of **pCOE$_{sp10}$**

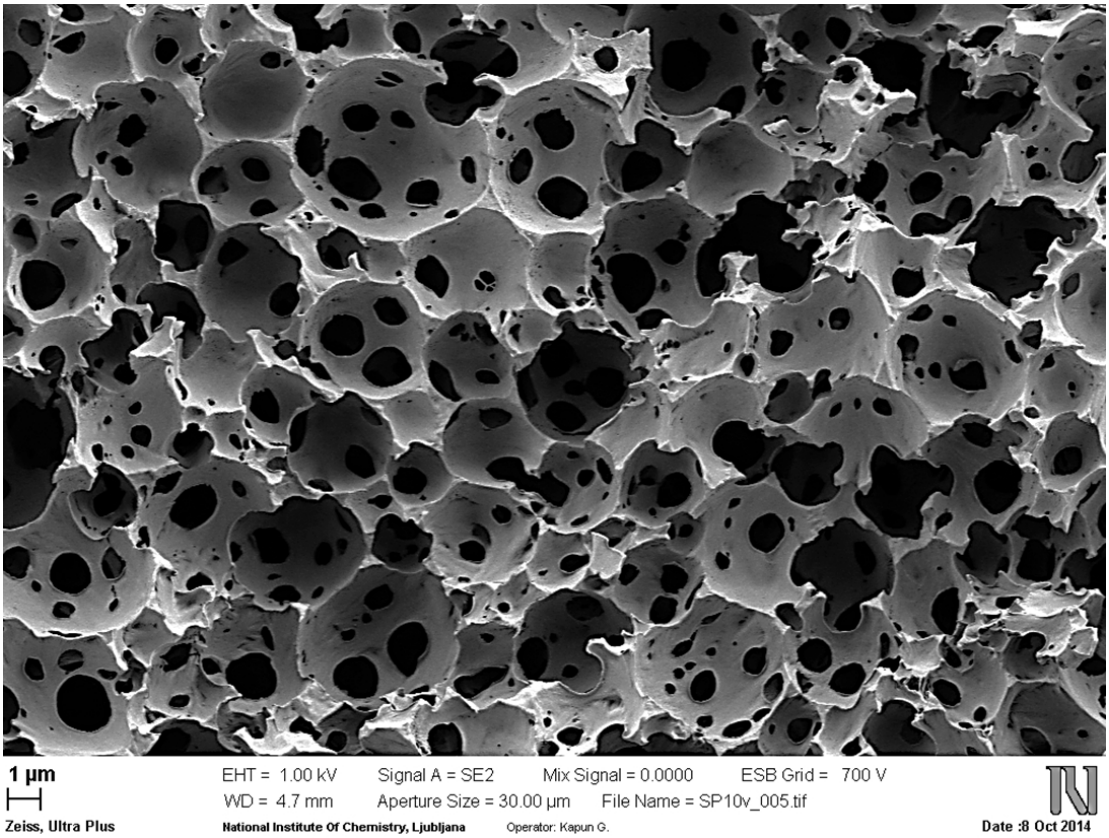

Figure S8. SEM image of **pCOE$_{sp10}$**

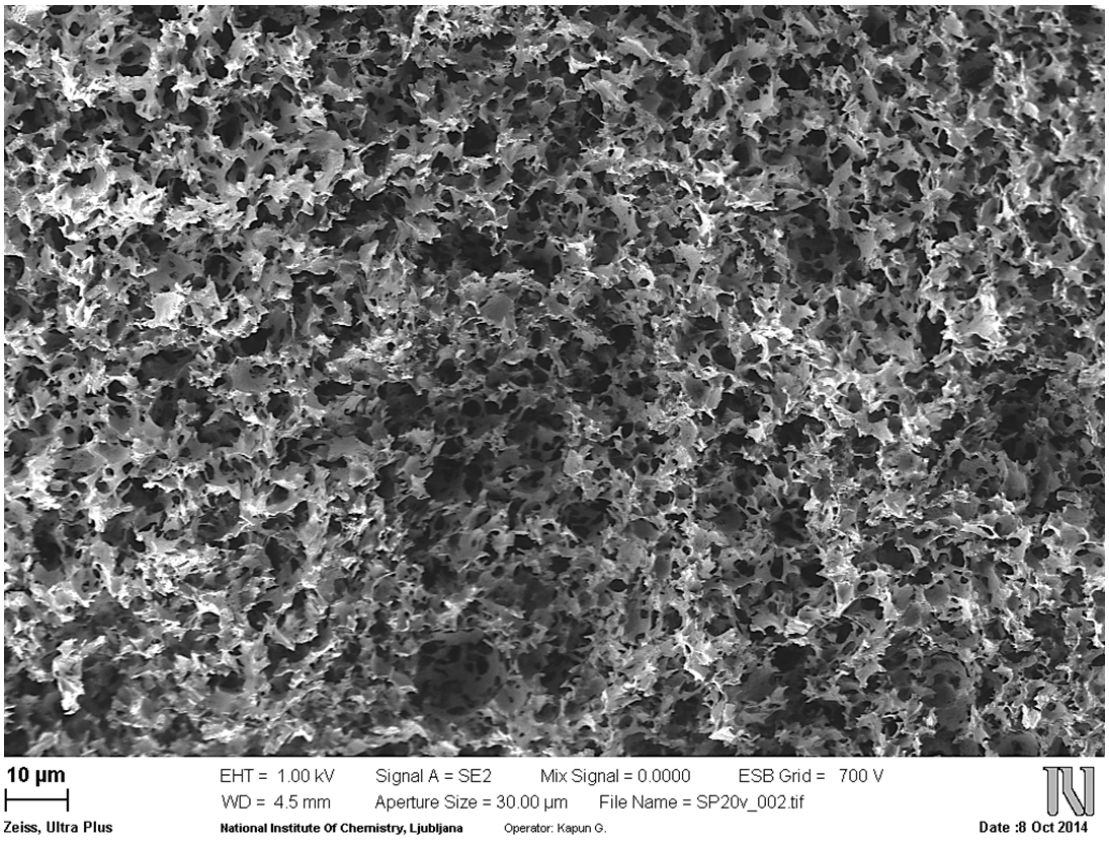

Figure S9. SEM image of **pCOE$_{sp20}$**

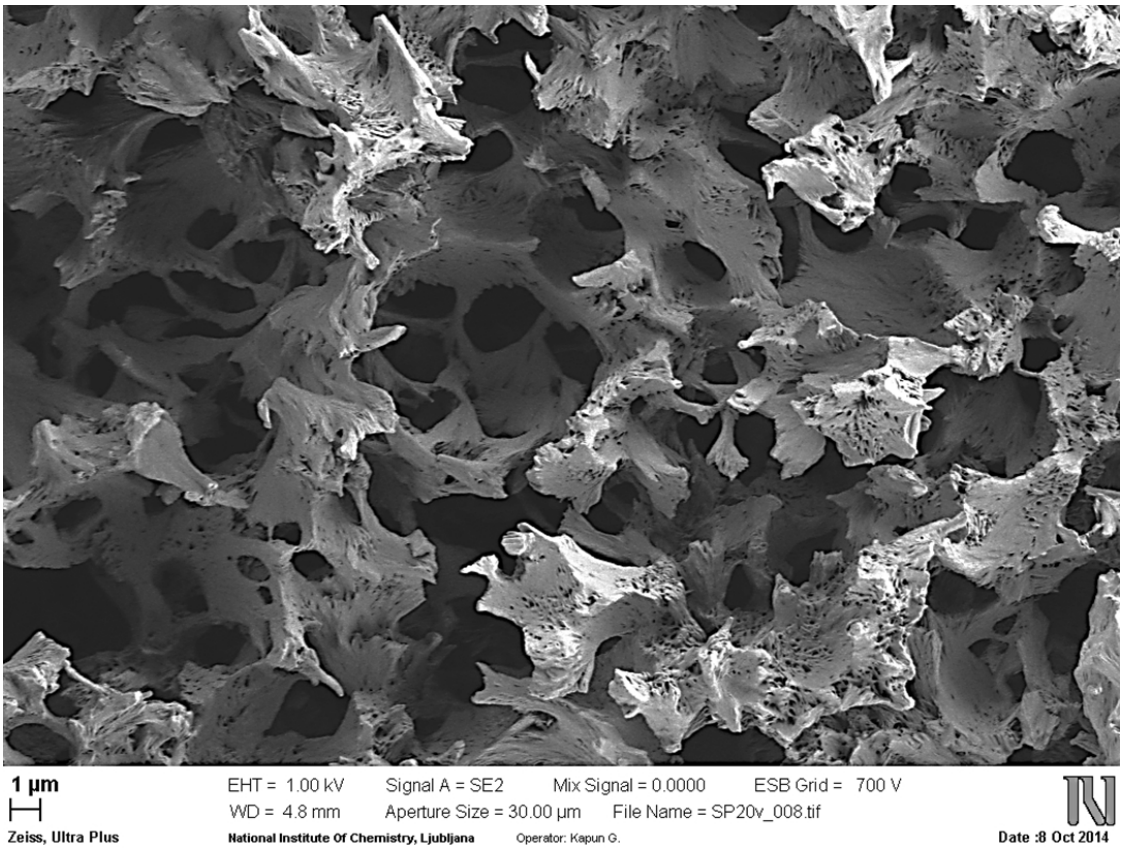

Figure S10. SEM image of **pCOE$_{sp20}$**

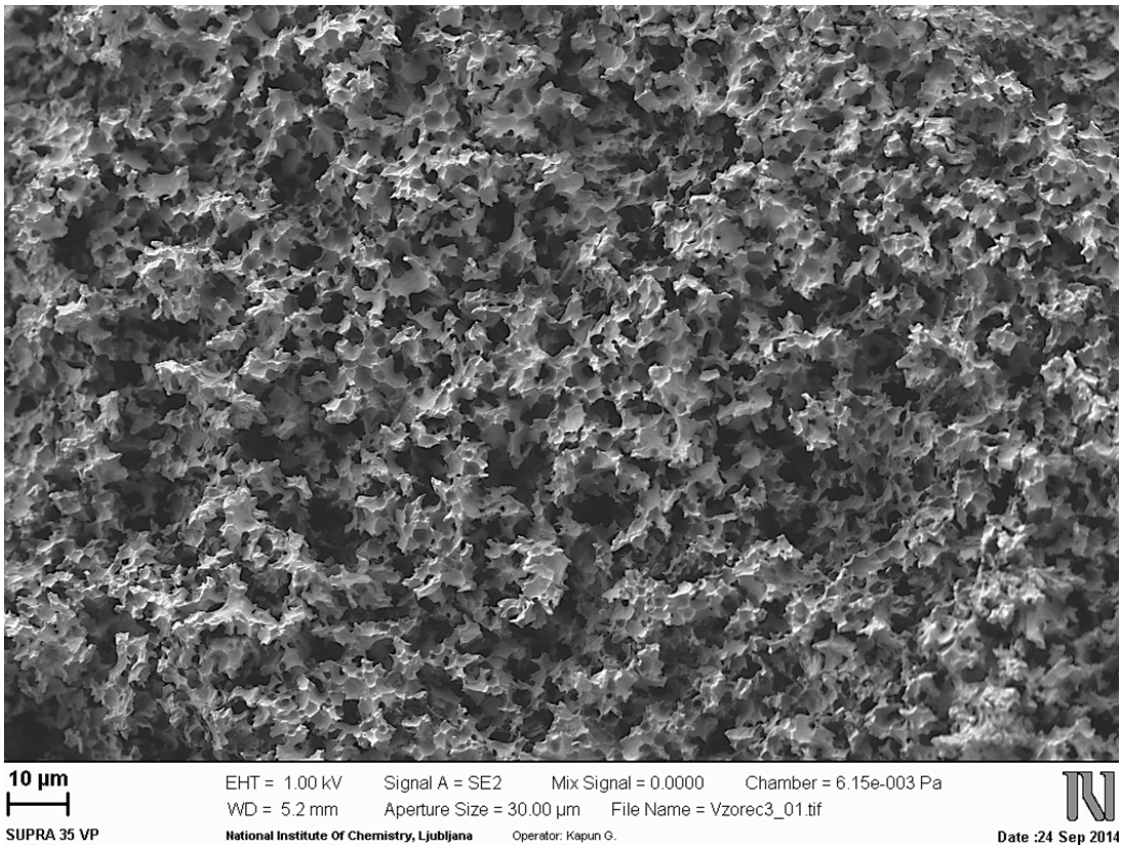

Figure S11. SEM image of **pCOE$_{sp30}$**

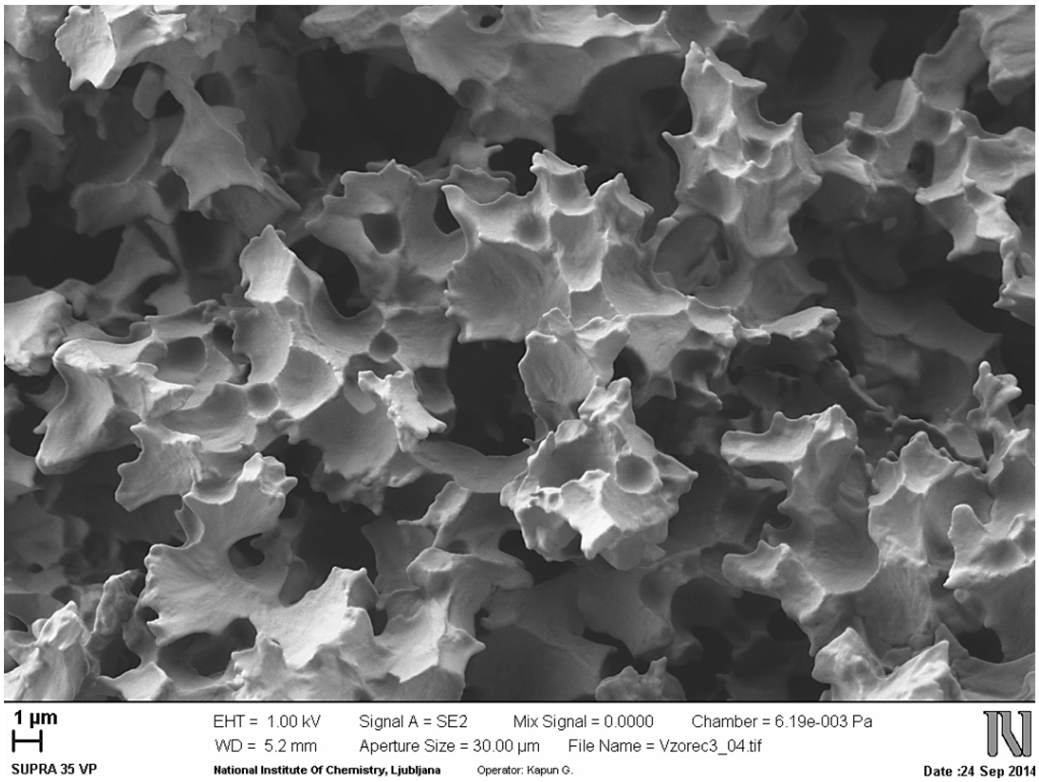

Figure S12. SEM image of **pCOE$_{sp30}$**

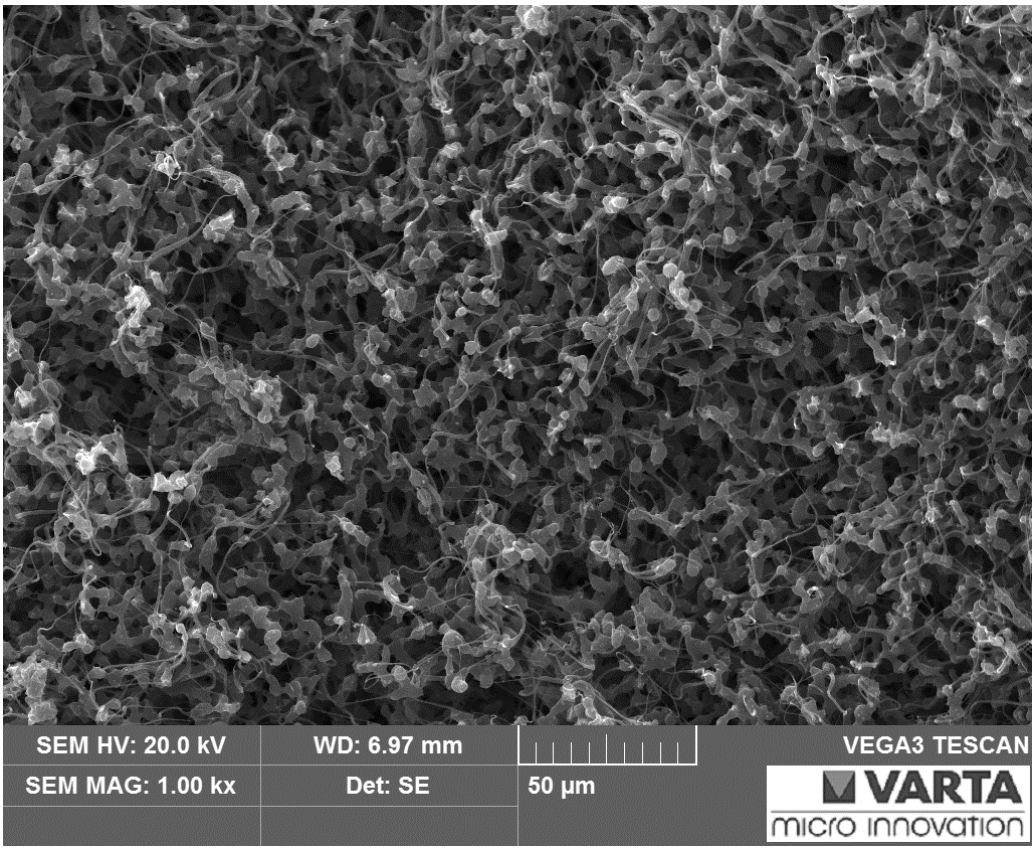

Figure S13. SEM image of **pCOE$_{pl}$**

Contact angle measurements

Measurements were performed as described elsewhere [Kovačič et al. *ACS Appl. Mater. Interfaces* 2014, **6**, 19075−19081]. Samples were prepared in the form of pellets between 2-4 mm in thickness by using tool-kit for the pellet preparation for FTIR measurements. The contact angle was than determined using the Krüss Drop Shape Analysis System.

Table S2. Contact angle (θ) values for pCOE samples.

Sample	Contact angle [°]			Mean value [°]
pCOE$_{sp10}$	71	70	70	70.3
pCOE$_{sp20}$	60	58	55	57.6
pCOE$_{sp30}$	72	69	68	69.6
pCOE$_{pl10}$	91	90	91	90.6

Imbibition experiment

Samples (**pCOE$_{sp20}$** and **pCOE$_{pl10}$**) were placed onto deionised water and were sonicated for 1h to facilitate the replacement of air for water. After this procedure the **pCOE$_{sp20}$** sample was found dipping just below the water surface while the **pCOE$_{pl10}$** sample swam on the water surface (Figure S14).

All pCOE HIPEs are light weight foams with skeletal densities of between 0.955 – 0.977 g/cm^3 (less than the water density) as determinate by the helium pycnometry. Accordingly, it is to expect that samples will not sink to the bottom of the vessel. However, after imbibition in water, the water obviously entered the pore system of the **pCOE$_{sp20}$** because the sample sunk below the water surface, supporting the hydrophilic character of the pores' surface because of the incorporation of Span 80 during HIPE curing.

The opposite is true for the **pCOE$_{pl}$** sample. In this case, the specimen remained swimming on the water surface. However, from the photographs it appears that half of the sample sunk below the water surface. This impression comes from the fact that it was sticking to the wall of the beaker or petri dish. After putting the **pCOE$_{pl10}$** specimen onto the water surface, it immediately started to swim towards the wall and stuck to it.

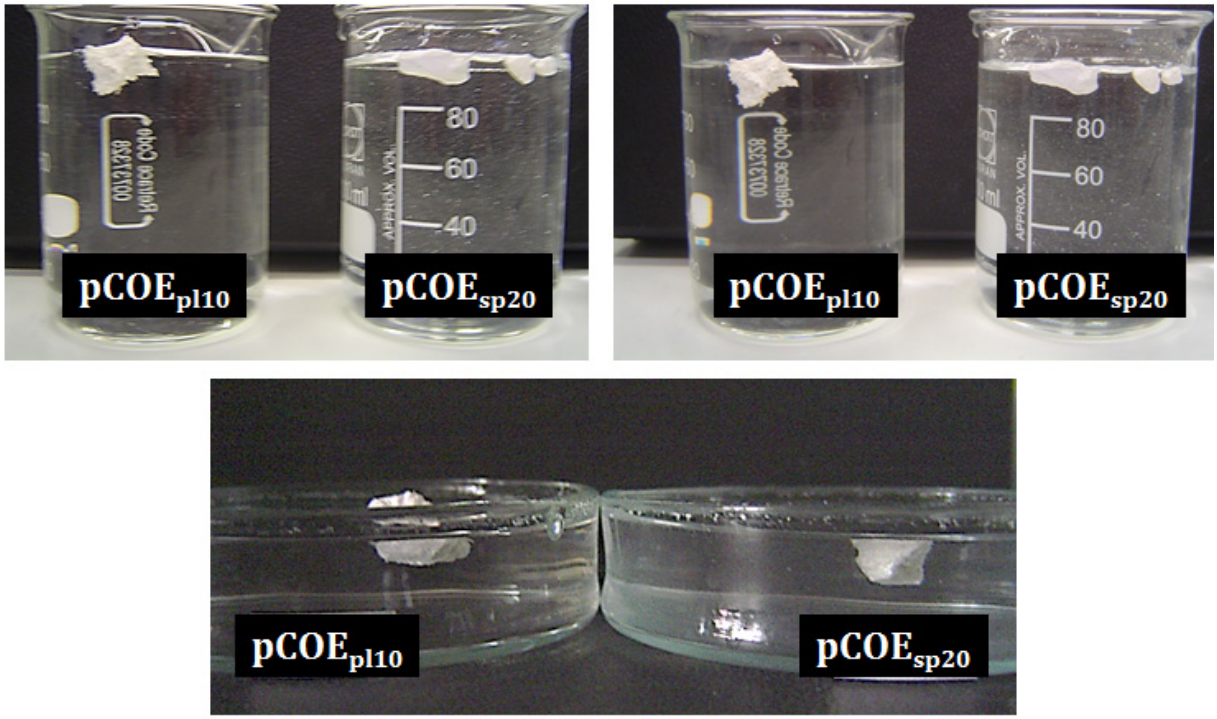

Figure S14. Photo images of **pCOE$_{sp20}$** and **pCOE$_{pl10}$** samples imbibed into the water in a beaker (above) and petri dish (below)